Journal of Sol-Gel Science and Technology (2020) 93:168–174
https://doi.org/10.1007/s10971-019-05146-5

ORIGINAL PAPER: NANO-STRUCTURED MATERIALS (PARTICLES, FIBERS, COLLOIDS, COMPOSITES, ETC.)

Check for updates

Nb_2O_5/SiO_2 mesoporous monoliths synthetized by sol–gel process using ammonium niobate oxalate hydrate as porogenic agent

Luiz Fernando de Sousa Lima[1] · Cintia Rodrigues Coelho[1] · Gustavo Henrique Magalhães Gomes[1] · Nelcy Della Santina Mohallem[1]

Received: 27 May 2019 / Accepted: 23 September 2019 / Published online: 8 October 2019

Abstract

Niobium pentoxide/silica mesoporous monoliths were prepared by using silicon alkoxide and a bifunctional reactant, ammonium niobate (V) oxalate hydrate (NbOXA), as niobium pentoxide precursor and porogenic agent. The influence of the thermal treatment on the structural, textural characteristics of the samples was evaluated. The thermal stability of the porous network was also evaluated. The introduction of the NbOXA in the silica sol–gel network promoted an increase in pore size diameter and in the total pore volume. The Nb_2O_5 nanoparticles were well dispersed inside the mesoporous silica matrix and their presence prevented the pore shrinking of the nanocomposite monolith at high temperatures, maintaining the total pore volume of the nanocomposites higher than those of the silica xerogels. To test the availability of the mesoporous nanocomposites as photocatalysts, they were submitted to UV light for methylene blue photobleaching, used as a model waste compound. Only the nanocomposite treated at 900 °C showed morphology and textural proprieties adequate to be photoactive.

Graphical Abstract

Silica/niobium pentoxide composite monoliths with high specific surface area and high pore volume in the range of mesopores, synthesized in one step with high dispersed nanoparticles inside the matrix.

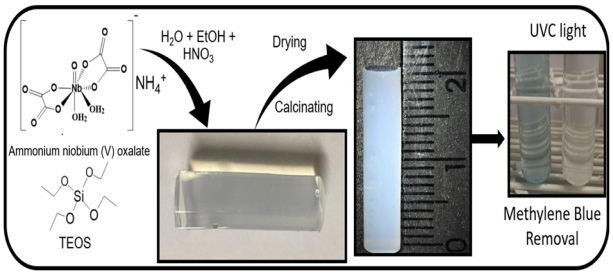

Highlights

1. Ammonium niobium (V) oxalate was used as porogenic agent in the preparation of monoliths of Nb_2O_5/SiO_2 mesoporous nanocomposites.
2. Nb_2O_5 nanoparticles were well dispersed inside the mesoporous silica matrix.
3. Nb_2O_5/SiO_2 nanocomposites were synthetized with high mesoporosity and good photocatalytic property.
4. The stability of the Nb_2O_5/SiO_2 mesoporous nanocomposites was confirmed by the high specific surface areas obtained at high calcination temperatures.
5. The Nb(V) octahedral coordination of the N_2O_5 nanoparticles formed inside the nanocomposites was elucidated by EELS.

Keywords Niobium pentoxide · Silica · Mesoporous materials · Nanocomposite · Sol–gel process · Photocatalyst

✉ Nelcy Della Santina Mohallem
nelcy@ufmg.br

[1] Laboratory of Nanostructured Materials, Chemistry Department, ICEx, Universidade Federal de Minas Gerais, Belo Horizonte, Brazil

1 Introduction

Materials based on niobium oxide polymorphs have currently attracted growing scientific and industrial interest, since Nb_2O_5 is a versatile semiconductor with application on electronic devices, sensors, and catalysis reactions like epoxidation, isomerization, dehydration [1, 3], and photocatalysis [4], among others. The use of Nb_2O_5 nanoparticles supported on porous silica matrices leads to an improvement in the catalytic activity and adsorptive capacity of the produced nanocomposites, due to the higher exposure of the reactive particle surfaces, increase of specific surface area, and formation of acid sites capable of catalyzing reactions [4–7].

The syntheses of those nanocomposites, usually obtained as powder, have required expensive chemicals (as niobium chloride or alkoxides) [6–8] and longtime synthesis [9]. The typical synthesis of this material is a two-step route, where a high specific surface area silica matrix is synthesized, and then impregnated with a precursor of niobium pentoxide, usually niobium (V) chloride [8], niobium (V) alkoxides [2, 10], or niobium (V) oxalate [11]. Another strategic synthesis is the conventional sol–gel route, where a silica source (silicon alkoxide or sodium silicate) is hydrolyzed in the presence of a niobium pentoxide source (niobium (V) chloride, or niobium (V) alkoxides) [7]. The polymorphism of niobium oxide is also a challenge for synthesizing this oxide. Depending on the conditions of synthesis and temperature of calcination, different phases can be achieved [7]. The stabilization of the active phases (Nb_2O_5) depends on the characteristics of the matrix support and the niobia precursor.

When compared with powders, nanocomposite monoliths obtained by sol–gel process have a more homogeneous structure, since the dispersion of pores is controlled during synthesis, the particle size distribution is often narrow and therefore the properties of the nanocomposite can be tailored [12]. The single structure of the monoliths allows faster mass transferring and lower pressure drops in flow systems (e.g., chromatography and flow reactors), leading to higher separation efficiency and consequently higher yields in reactions [8]. This kind of material can also be used in the construction of sensors, detectors, and molecular sieves.

The aim of this work is to produce a one-step synthesis of Nb_2O_5/SiO_2 nanocomposite using a route that lead to monoliths, combining the conventional sol–gel process with the thermal decomposition of a stable chelate of niobium (V) (niobate oxalate hydrate), used as source of Nb_2O_5 and porogenic agent. This process allows the control of the niobia structure, the specific surface area and the porosity, generating nanocomposites with good nanoparticle dispersion and photocatalytic activity.

2 Experimental

Pure silica xerogel monoliths were synthesized by mixing tetraethyl orthosilicate (TEOS -Sigma-Aldrich 98%), ethanol and water in a molar proportion of 1:3:10, respectively. The hydrolysis was performed under acidic pH (~2), controlled with nitric acid, and the system was under vigorous stirring for 2 h. After aging for 2 h at 60 °C in sealed tubes, the gels were dried at 60 °C for 72 h and 110 °C for 12 h to eliminate all the solvent. Posteriorly, the monoliths were calcined at 500, 700, 900, and 1100 °C for 3 h. The nanocomposite monoliths were prepared by addition of ammonium niobate (V) oxalate hydrate (NbOXA - $NH_4[NbO(H_2O)_2(C_2O_4)_2].xH_2O$) dried in oven at 120 °C for 12 h to eliminate adsorbed water, with molar proportions of Si:Nb = 1:0.1 (10%) and 1:0.05 (5%), following the same procedure of the pure silica.

The thermal stability studies in this temperature range help us understanding how the presence of niobate oxalate hydrate (NbOXA) changes the silica matrix textural properties, working as porogenic agent, to produce the monoliths with good porosity and high surface area.

The NbOXA was thermally characterized (TG/DTA) in an equipment STAR^e system by Mettler Toledo, accompanied by X-ray diffraction (Shimadzu XRD-7000) and Fourier transform infrared (FTIR) (Perkim Elmer BX), to determine its structural behavior under different temperatures. The structural characteristics of the silica matrix and of the nanocomposites were evaluated by XRD and their microstructure and morphology were investigated by high resolution transmission electron microscopy (HRTEM—SuperTwin FEI/200 kV) with electron coupled energy loss spectroscopy (EELS). Specific surface area and porosity were evaluated by N_2 gas adsorption technique (QuantaChrome/NOVA 1200e), using BET and BJH methods, respectively.

Methylene blue (MB) photobleaching was used to evaluate the applicability of the materials as photocatalysts. Aliquot of 0.5 g of each material was add to 25 mL of MB solution (12 ppm) and kept in a dark chamber for 2 h. After that, a lamp with UVC light (Phillips/254 nm) was switched on and samples were collected every 30 min. The photobleaching performance was evaluated measuring the absorbance reduction (C/C^0), by UV–vis spectroscopy (Agilent/Cary 100 spectrophotometer), over time.

3 Results and discussion

3.1 NbOXA decomposition

The behavior of the NbOXA as a function of the temperature helps understanding the subsequent phenomena of the

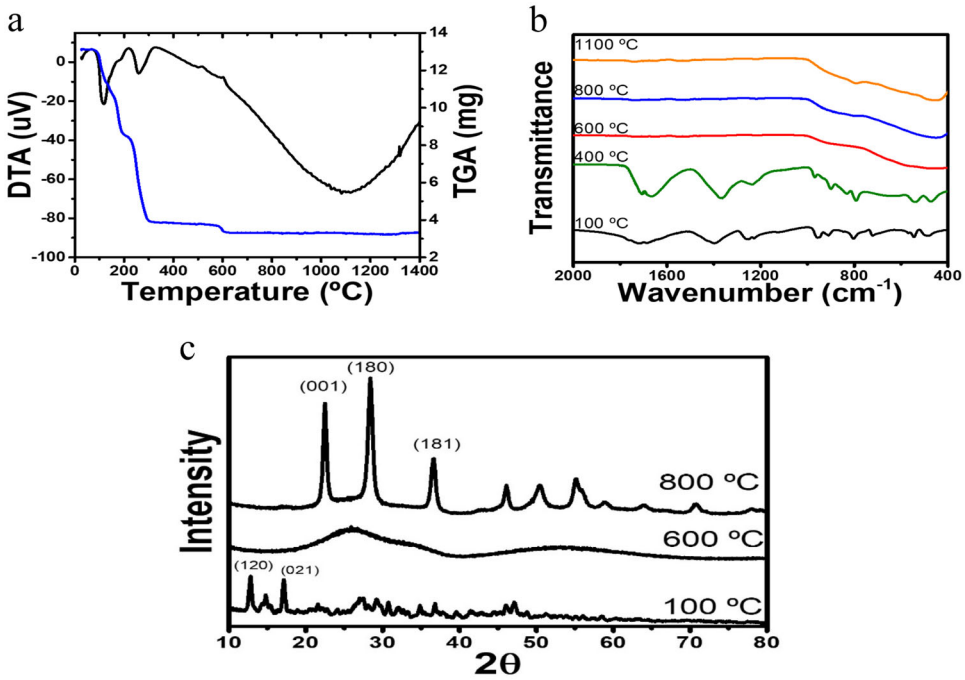

Fig. 1 **a** TG/DTA, **b** FTIR spectra, and **c** XRD of NbOXA treated at several temperatures (orthorhombic phase obtained at 800 °C)

niobium pentoxide formation inside the silica matrix. The TG/DTA curves (Fig. 1a) shows a weight loss of ~40% until 190 °C due to remove of adsorbed and structural waters. The decomposing of organic matter occurs until 590 °C with weight loss of 50% and formation of the niobium pentoxide. The small loss of mass from 590 °C to 600 °C can be attributed to desorption of CO_2 and dehydration of niobic acid leading to the final structure of niobium pentoxide. The results are in accordance with ones reported by other authors [13], and are supported by the XRD and FTIR of the NbOXA calcined at different temperatures (Fig. 1b, c).

The FTIR spectra (Fig. 1b) show that even when submitted at temperature of 400 °C the carboxylic groups are still present, confirmed by the bands at 1700 cm^{-1} (C=O stretching) and 1380 cm^{-1} (C–O asymmetrical stretching). The absence of those bands in the sample treated at 600 °C can be attributed to the beginning of the formation of Nb_2O_5 at 590 °C, indicating the decomposition of the ammonium niobite (V) oxalate hydrate. The large and round bands at 600, 800, and 1100 cm^{-1} are relative to Nb–O stretching and out of plane distortions [1, 3]. Figure 1c shows characteristic patterns of NbOXA (card 83–1993), whose crystalline structure collapses due to the heating process with the loss of carboxylic groups. A new organization of the structure occurs around 600 °C (Fig. 1b), leading to the formation of the orthorhombic Nb_2O_5 phase (card 30–873) at 800 °C.

3.2 Xerogel and composites structure

The monoliths, silica xerogel and nanocomposites, were obtained without cracks, due to the controlled drying process. The silica xerogel became transparent, the nanocomposites became white, and the silica xerogel showed a shrinkage rate higher than the nanocomposite. Silica monoliths did not show diffraction peaks, as expected to noncrystalline materials (Fig. 2). The nanocomposites also did not present any crystalline structure at low temperature, while at 900 °C the diffractogram shows the presence of Nb_2O_5 orthorhombic (peaks $2\theta = 22$, 28, 36, 46°/card 30–873) and monoclinic phases (shoulder at $2\theta = 25$°/card 30–871). At 1100 °C remain only the orthorhombic phase and the peaks at $2\theta = 21$ and 31° shows that the silica is structuring as cristobalite. These results suggest that the Nb_2O_5 nanoparticles inside the silica matrix induces the crystallization of the silica at lower temperatures, acting as nucleating points for topotaxial growth of cristobalite.

Although XRD patterns of the sample heated at 500 °C did not show any evidences of crystalline niobium pentoxide, due to the technique sensibility, crystallites of 3 nm with interplanar spacing of 3.9 Å, related to (001) planes of the orthorhombic phase could be detected by HRTEM inside the porous matrix (Fig. 3a). For samples annealed at 700 °C (Fig. 3b), the nanoparticles grew, reaching an average size of 6 ± 2 nm. When the samples were annealed at 900 °C (Fig. 3c), the nanoparticles of niobium pentoxide

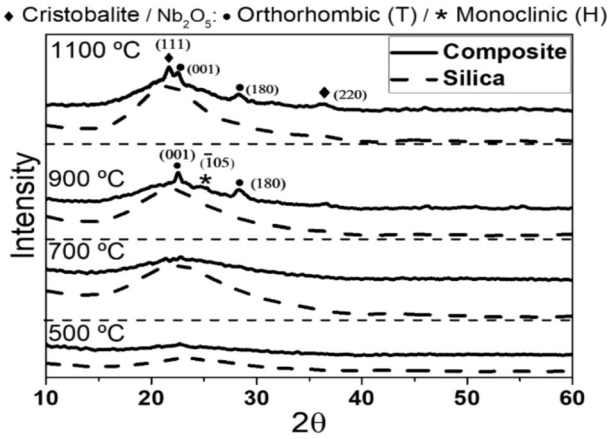

Fig. 2 XRD patterns of silica and silica/niobium pentoxide xerogels (10%) calcinated at 500, 700, 900 (peaks of orthorhombic (•) and monoclinic phases (*) of niobium pentoxide) and 1100 °C (peaks of orthorhombic (•) niobium pentoxide and cristobalite (♦)

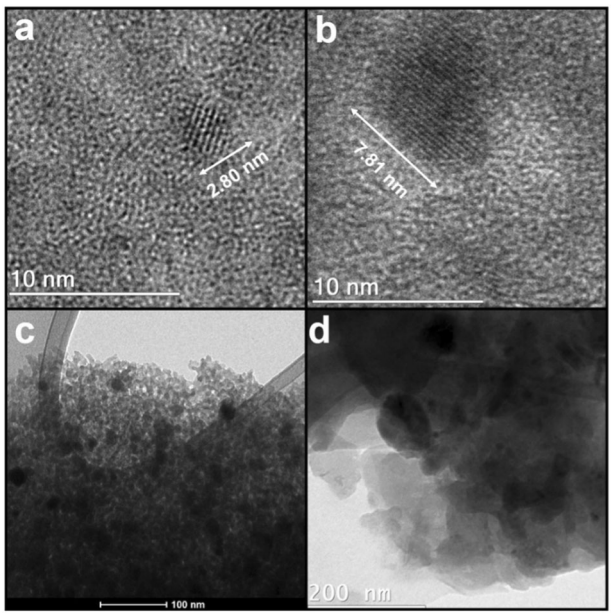

Fig. 3 Transmission electron microscopy images of composites silica/niobium pentoxide (10%) calcinated at 500 (**a**), 700 (**b**), 900 (**c**), and 1100 °C (**d**)

reached 16 ± 5 nm, remaining well dispersed into the porous matrix. The silica appeared as a dense glass and the Nb_2O_5 nanoparticles were encapsulated for samples calcined at 1100 °C (Fig. 3d). The diffractograms of the nanocomposites (5%) were similar to those of nanocomposites (10%), with less intense peaks.

EELS was performed (Fig. 4) to determine the composition and phase of the niobium pentoxide nanoparticles in nanocomposite 10% niobium treated at 500 °C.

The spectra show niobium edges Nb $M_{4,5}$ at 210 eV, duplet $M_{2,3}$ at 363 and 378 eV, and O duplet K around 530 eV,

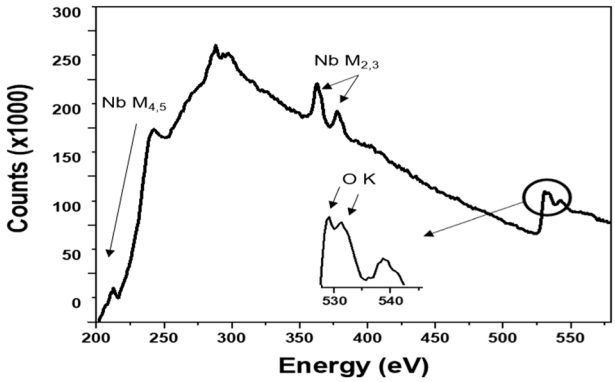

Fig. 4 EELS spectra of silica/niobium pentoxide nanocomposite (10%) calcined at 500 °C

which can identify the crystallites as niobium pentoxide [14, 15]. The edge Nb $M_{4,5}$ is associated to 3d–4f and 3d–5p transitions, and the duplet Nb $M_{2,3}$ is related to transitions from 3p orbitals to 4d and 5s unoccupied orbitals [15].

The oxygen K edge appearing as a duplet instead of a singlet is an evidence of the coordination number of the niobium (V). This edge is explained by transitions from 1s electrons to 2p unoccupied states. By the ligand-field theory, the niobium pentoxide octahedrally coordinated by the oxygens, as in the Nb_2O_5 (where NbO_6 octahedral structures shares corners and/or edges to form different unitary cells [16]), splits its 4d orbitals into e_g (higher energy) and t_{2g} (lower energy) orbitals. This two set of orbitals are bonded with oxygen 2p orbitals, the t_{2g} orbitals overlapping with oxygen 2p orbitals generated the first peak, and the second peak appears as the e_g orbital overlaps with oxygen 2p orbitals [15]. The 3.5 eV value, which is the distance between the peaks of the duplet is coherent with the range of the band gap of Nb_2O_5.

These experiments evidence that the decomposition of NbOXA initially leads to amorphous niobium pentoxide homogeneously dispersed inside the silica matrix. The increase in temperature of calcination provokes a thermal diffusion process, favored by the matrix porosity, leading to crystallization and growth of these nanoparticles until their encapsulating by silica at 1100 °C.

3.3 Textural properties

Silica xerogel and nanocomposite (10%) adsorption–desorption isotherms as a function of the calcination temperature are shown in Fig. 5a, b and the respective pore size distribution are shown in Fig. 5c, d. The textural characteristics obtained by BET and BJH theories are shown in Table 1. The C constant shows that the measurements are reliable in the selected range ($0.05 < P/P_o < 0.3$) [17].

The hysteresis of the silica xerogel monoliths calcined at temperatures between 500 and 900 °C are due capillary

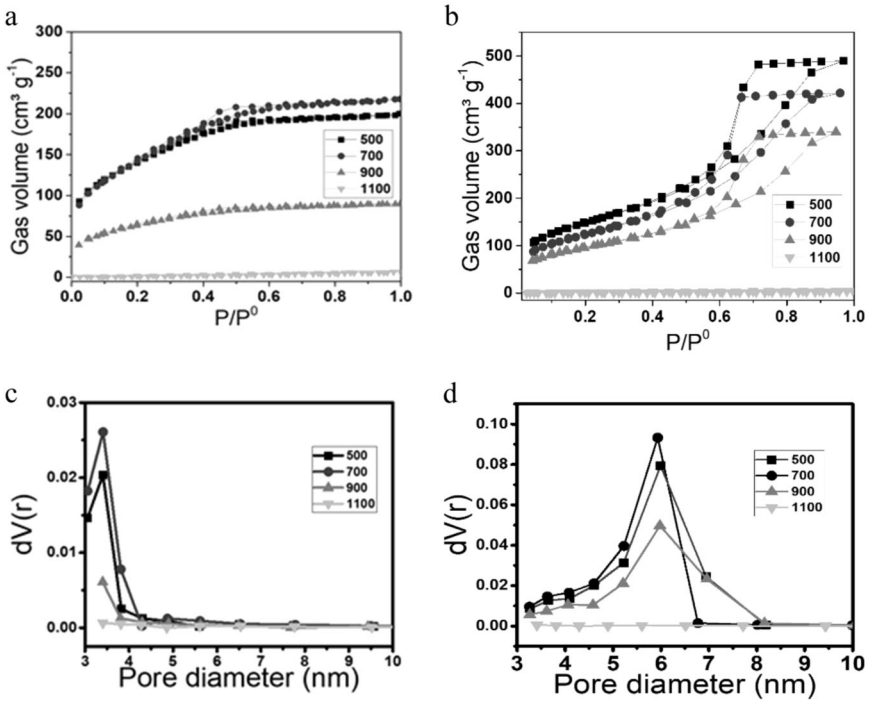

Fig. 5 Nitrogen adsorption isotherms of silica (**a**) and nanocomposites (10%) (**b**) xerogels calcinated at 500, 700, 900, and 1100 °C. Pore size distribution by B.J.H of silica (**c**) and nanocomposites

Table 1 Textural properties of silica and nanocomposites (10%) calcinated at temperatures of 500, 700, 900, and 1100 °C

Sample/	Temperature °C	SSA ($m^2\ g^{-1}$)	*C*	r^2	Average pore diameter (nm)	Total pore volume[a] ($cm^3\ g^{-1}$)
Silica/	500	489	240	0.9995	2.6	0.35
	700	511	96	0.9998	2.6	0.34
	900	223	153	0.9995	1.3	0.14
	1100	0	<0	0.8637	–	–
Nanocomposite/	500	530	118	0.9999	6.0	0.76
	700	445	96	0.9999	6.0	0.75
	900	344	111	0.9999	5.8	0.65
	1100	3	4	0.8272	–	–

[a]Measured at adsorption saturation point ($P/P^0 = 0.98$)

condensation on pores surface and are typical of mesoporous materials with small pore size, around 2.6 nm, near the limit of micropore size, that is below 2.0 nm [17]. The silica xerogel annealed at 700°C showed the highest A_{BET} and the small hysteresis is due to cavitation of the material during the desorption process. After calcination at 900 °C, the cavitation process reduces due to the densification process of the xerogel, making the hysteresis almost undetectable, and the A_{BET} diminishes. At 1100 °C, the densification is complete and the xerogel does not adsorb nitrogen. The presence of NbOXA modifies the types of the nanocomposite isotherms and the samples treated between 500 and 900 °C present isotherms characteristics of mesoporous material (type IV) [17] with average porous size between 5.8 and 6.0 nm, suggesting that the NbOXA adsorbed at the gel skeleton works as a pore directing agent. The presence of NbOXA in xerogel causes an increase in volume of adsorbed N_2 and in the average pore size, as well as changes in the A_{BET} of the samples calcined at 500 and 700 °C.

Nanocomposites prepared at 900 °C showed A_{BET} higher than the silica xerogel, suggesting that Nb_2O_5 nanoparticles formed by thermal decomposition generated inside the monolith pores stabilizes the matrix structure, preventing their contraction at high calcination temperatures. It is well known in the literature that some oxides [18, 19] gives thermal stability to the silica porous structure, retarding the material densification. The pores of the nanocomposite heated at 1100 °C collapse and no nitrogen is adsorbed, suggesting that the niobium pentoxide is encapsulated inside the silica matrix.

The SSA, porosity, and average pore diameter values of the nanocomposite 5% niobium were similar to the nanocomposite 10% niobium ones, and therefore, these results are not being presented here.

The SSA, the average pore diameter and the total pore volume of silica xerogel reduces when the temperature of calcinating is increased, by viscous sintering [18]. At this process, the viscous flow of the amorphous silica shrinks its pores and reduces SSA to reduce surface tensions.

Part of the shrinkage of the silica, by viscous sintering, is attributed to condensation of silanol groups on vicinal particles [18]. The niobium pentoxide on the surface of the silica skeleton prevents this condensation by blocking the silanol groups, preventing the reduction of the SSA and pore shrinkage [19]. At the temperature of 1100 °C both the silica and composite are completely densified.

The SSA obtained for the nanocomposite calcinated at 500 °C (530 m^2g^{-1}) is higher than the 430 m^2g^{-1} obtained by classic sol–gel route [7] or 295 m^2g^{-1} using the impregnation method over MCM-41 [9], and 500 m^2g^{-1} by impregnation method using SBA-15 as silica matrix [20], as shown in Table 2. There is a lack of information to compare the behavior of the composite SSA under different temperatures.

3.4 Photoactivity

As expected, the pure silica xerogel treated at any temperatures did not show photoactivity. The nanocomposites treated at 500 and 700 °C are formed by small crystallites with low photoactivity dispersed inside the matrix, while the samples heated at 900 °C presented good activity, reducing the concentration of MB in 80% after 500 min, with a performance proportional to the amount of niobium load inside the monolith. Figure 6 shows the reduction at the concentration of MB over time, during the exposition of the system to UVC light.

The model considers an apparent first-order equation because the concentration of the dye is in the range of ppm, where C_0 is the initial concentration of the dye, C is the concentration at each time t, and K_{ap} is the apparent kinetic constant of a pseudo-first order reaction.

$$ln\frac{C_0}{C} = K_{ap}t$$

The plot of C_0/C against time of the MB in the presence of the nanocomposites with 5% and 10% of Nb is inserted in Fig. 6. The R^2 of the adjustment is 0.9965 for the 10% and 0.9987 for the 5%, indicating that the kinetic of the MB photobleaching can be approached to the Langmuir–Hinshelwood model.

The adjusted equations gave an apparent constant of 0.00341 and 0.00235, for the samples with 10 and 5% of Nb:Si, showing that increasing the niobium load in the nanocomposite increases its photoactivity, since the niobium pentoxide is the photoactive phase. Although nanocomposite 5% niobium has approximately the same textural characteristics as nanocomposite 10% niobium, its performance is inferior probably due to the lower number of active sites. However, the Nb_2O_5 powder obtained by thermal decomposition and calcined at 900 °C did not show photoactivity. This result shows the potentiality of the nanocomposite as a photocatalyst to be used at high temperatures.

The nanocomposites treated between 500 and 900 °C adsorbed well the MB of the solution, while the ones sintered at 1100 °C were not able to either adsorb or photobleach the MB.

In the nanocomposites treated at 900 °C, the niobium pentoxide particles have adequate size and free surface to proceed with the interfacial electron transfer mechanism, where the electrons at the valence band are excited by the

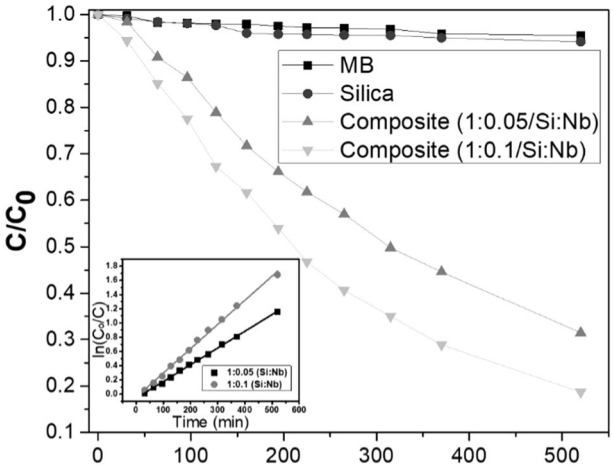

Fig. 6 MB photobleaching under UVC light in the presence of silica/niobium pentoxide composites (1:0.05 and 1:0.1/Si:Nb) and silica

Table 2 Specific surface area (SSA) of Nb_2O_5/SiO_2 composites obtained by different routes

Synthesis method	Nb_2O_5 precursor	SSA ($m^2\,g^{-1}$)	Reference
Classic sol–gel	$NbCl_5$	430	[7]
Impregnation	Niobium (V) ethoxide	295	[9]
Impregnation	$NbCl_5$	500	[20]
Sol–gel and thermal decomposition	Ammonium niobate oxalate hydrate	530	Present work

photons, producing pair electron–hole that can be transferred to the chemicals surrounding the surface of the material, before recombining [21]. The sample treated at 1100 °C, on the other hand, has the niobium pentoxide particles encapsulated by the sintered silica matrix, and neither electrons nor holes generated by the irradiation can be transferred to the particle surroundings, as silica is an insulation material, making it impossible to the niobium pentoxide to bleach the dye.

4 Conclusions

Monolithic Nb_2O_5/SiO_2 nanocomposites were produced with high surface areas and the niobium pentoxide characterized by EELS spectra showed octahedral coordination with oxygens, precisely by the O K edges.

The ammonium niobate (V) oxalate hydrate worked as a porogenic agent, changing the textural properties of the silica xerogel monoliths, increasing the mesopore sizes, the porosity and the capacity of adsorption of the nanocomposite. The proposed method produced nanocomposites with Nb_2O_5 nanoparticles highly dispersed inside the silica matrix, whose size increased with the temperature of preparation. The niobium pentoxide formed by in-situ decomposition at 900 °C in silica xerogel matrix had particle size (~16 nm), porosity and specific surface area adequate to originate a nanocomposite promisor as sensor and photocatalyst at high temperature, maintaining the structural stability of the silica porous network. The presence of the niobium pentoxide induced the crystallization of the amorphous silica xerogel to cristobalite at lower temperatures than the usual phase transformation temperature of conventional silica.

Acknowledgements This work was supported by CNPq, CAPES, and FAPEMIG (Brazilian agencies). The authors acknowledge Center of Microscopy at UFMG for the infrastructure.

Compliance with ethical standards

Conflict of interest The authors declare that they have no conflict of interest.

References

1. Brandão RF, Quirino RL, Mello VM, Tavares AP, Peres AC, Guinhos F et al. (2009) Synthesis, characterization and use of Nb_2O_5 based caalysts in producing biofuels by transesterification, esterification and pyrolysis. J Braz Chem Soc 20:954–66
2. Turco R, Aronne A, Carniti P, Gervasini A, Minieri L, Pernice P et al. (2015) Influence of preparation methods and structure of niobium oxide-based catalysts in the epoxidation reaction. Catal Today 254:99–103
3. Athar T, Hashmi A, Al-Hajry A, Ansari ZA, Ansari SG (2012) One-pot synthesis and characterization of Nb2O5 nanopowder. J Nanosci Nanotechnol 12:7922–6
4. Jaramillo-Páez C, Sánchez-Fernández FJ, Navío JA, Hidalgo MC (2018) Photo-induced processes on Nb 2 O 5 synthesized by different procedures. J Photochemistry Photobiol A: Chem 359:40–52
5. Ziolek M, Sobczak I (2017) The role of niobium component in heterogeneous catalysts. Catal Today 285:211–25
6. Umpierres CS, Prola LD, Adebayo MA, Lima EC, Dos Reis GS, Kunzler DD et al. (2017) Mesoporous Nb2O5/SiO2 material obtained by sol-gel method and applied as adsorbent of crystal violet dye. Environ Technol 38:566–78
7. Francisco MSP, Gushikem Y (2002) Synthesis and characterization of SiO2–Nb2O5systems prepared by the sol–gel method: structural stability studies. J Mater Chem 12:2552–8
8. Anilkumar M, Hoelderich WF (2012) Gas phase Beckmann rearrangement of cyclohexanone oxime to ε-caprolactam over mesoporous, microporous and amorphous Nb2O5/silica catalysts: a comparative study. Catal Today 198:289–99
9. Gao X, Wachs IE, Wong MS, Ying JY (2001) Structural and reactivity properties of Nb MCM-41: comparison with that of highly dispersed Nb2O5/SiO2 catalysts. J Catal 203:18–24
10. Yoshida H, Tanaka T, Yoshida T, Funabiki T, Yoshida S (1996) Control of the structure of niobium oxide species on silica by the equilibrium adsorption method. Catal Today 28:79–89
11. He J, Li Q-J, Fan Y-N (2013) Dispersion states and acid properties of SiO2-supported Nb2O5. J Solid State Chem 202:121–7
12. Sachse A, Galarneau A, Coq B, Fajula F (2011) Monolithic flow microreactors improve fine chemicals synthesis. New J Chem 35:259
13. Su TT, Zhai YC, Jiang H, Gong H (2009) Studies on the thermal decomposition kinetics and mechanism of ammonium niobium oxalate. J Therm Anal Calorim 98:449
14. Bach D, Schneider R, Gerthsen D, Verbeeck J, Sigle W (2009) EELS of niobium and stoichiometric niobium-oxide phases—Part I: plasmon and near-edges fine structure. Microsc Microanalysis 15:505–23
15. Bach D, Störmer H, Schneider R, Gerthsen D, Verbeeck J (2006) EELS investigations of different niobium oxide phases. Microsc Microanal 12:416–23
16. Nico C, Monteiro T, Graça MPF (2016) Niobium oxides and niobates physical properties: review and prospects Prog Mater Sci 80:1–37
17. Thommes M, Kaneko K, Neimark AV, Olivier JP, Rodriguez-Reinoso F, Rouquerol J et al. (2015) Physisorption of gases, with special reference to the evaluation of surface area and pore size distribution (IUPAC Technical Report). Pure Appl Chem 87:1051–69
18. Brinker CJ, Scherer GW (1990) Sol-Gel Science: the physics and chemistry of sol-gel processing. Academic Press, San Diego, CA
19. de Sousa EM, de Sousa AP, Mohallem ND, Lago RM (2003) Copper-silica sol-gel catalysts: structural changes of Cu species upon thermal treatment. J Sol-Gel Sci Technol 26:873–7
20. Silva Â, Wilson K, Lee AF, dos Santos VC, Cons Bacilla AC, Mantovani KM et al. (2017) Nb 2 O 5 /SBA-15 catalyzed propanoic acid esterification. Appl Catal B: Environ 205:498–504
21. Liu B, Zhao X, Terashima C, Fujishima A, Nakata K (2014) Thermodynamic and kinect analysis of heterogeneous photocatalysis for semiconductor systems. Phys Chem Chem Phys 16:8751–60